Quantum weak and modular values in enlarged Hilbert spaces

Le Bin Ho* and Nobuyuki Imoto
Graduate School of Engineering Science, Osaka University, Toyonaka, Osaka 560-8531, Japan

(Received 23 October 2017; published 16 January 2018)

We introduce an enlarged state, which combines both pre- and postselection states at a given time t in between the pre- and postselection. Based on this form, quantum weak and modular values can be completely interpreted as expectation values of a linear combination of given operators in the enlarged Hilbert space. This formalism thus enables us to describe and measure the weak and modular values at any time dynamically. A protocol for implementing an enlarged Hamiltonian has also been proposed and applied to a simple example of a single spin under an external magnetic field. In addition, the time-dependent weak and modular values for pre- and postselection density matrices mapping onto an enlarged density matrix are also discussed.

DOI: 10.1103/PhysRevA.97.012112

I. INTRODUCTION

Traditionally, it is believed that the state of a system at time t ($>t_i$: the initial time) is solely determined by the initial condition at time t_i, both for classical mechanics and quantum mechanics. In this context, the final condition is not relevant as it is merely the result of the natural evolution of the system. Recently, however, people started to consider such cases where the final state at time t_f ($>t$) is postselected via a projection measurement. In this case, the final state plays a role of the posterior condition and affects, together with the initial state, the statistics of the observed values. Thus the initial and final states are equally important to give a complete description of the quantum system [1]. Such kind of theory is known as the two-state vector formalism (see pp. 1–8 of Ref. [2] and Chap. 13 of Ref. [3]).

The concepts of quantum weak values [4] and, very recently, quantum modular values [5] are given in the two-state vector formalism,

$$\langle \boldsymbol{A}\rangle_{\rm w} = \frac{\langle\phi|\boldsymbol{A}|\psi\rangle}{\langle\phi|\psi\rangle} \text{ and } (\boldsymbol{A})_{\rm m} = \frac{\langle\phi|e^{-ig\boldsymbol{A}}|\psi\rangle}{\langle\phi|\psi\rangle}, \qquad (1)$$

where $\langle \boldsymbol{A}\rangle_{\rm w}$ ($(\boldsymbol{A})_{\rm m}$) is the weak (modular) value of an observable $\boldsymbol{A}$ with the pre- and postselected states $|\psi\rangle$ and $|\phi\rangle$, corresponding to the initial and the final conditions, respectively. Here, the constant g can take any real value. Weak and modular values are related to each other through g [5,6]. Both of them are found to be useful in explaining many phenomena such as quantum paradoxes [7–14], quantum ergodicity [15], and many applications in amplification and precision metrology [16–20].

A weak value can be obtained by weak measurements [4,21,22], whereas a modular value can be obtained by arbitrarily strong measurements [5]. In any case, the time t when the measurement is done does not matter if the system stays in the same state during $t_i \leqslant t \leqslant t_f$. If the state evolves, however, we should use $|\psi(t)\rangle$ and $|\phi(t)\rangle$ in Eq. (1) instead of $|\psi\rangle$ and $|\phi\rangle$, where $|\psi(t)\rangle$ is the evolution of $|\psi\rangle$ from t_i to t and $|\phi(t)\rangle$ is the backward evolution of $|\phi\rangle$ from t_f to t. This new expression, however, does not mean that the weak value (or the modular value) is expressed as a dynamical evolution. To obtain a weak (or modular) value at time t, we need to prepare $|\psi\rangle$ at time t_i, wait until t_f, and postselect $|\phi\rangle$ at time t_f, for each choice of t.

It is, however, desirable if we can construct a different set of a large system that can simulate the original set of the system in such a way that the new system is not postselected at time t_f. In this case, the time-dependent (but not dynamically evolving) weak value is simulated by an expectation value of the new system that simply evolves in one direction from its initial condition at t_i.

One possible method to do so might be the use of a "generic two state," which is a direct product of a *ket* vector and a *bra* vector [1,23,24]. This generic-two-state description, however, simply gives a convenient form for a weak value rather than describes it as the initial-condition problem. Recently, a two-time state or a process matrix was introduced, wherein the preselection state is entangled with the postselection state [25]. The process matrix formalism also has connected with the "indefinite causal order" and can be simulated in quantum mechanics by using postselections [26].

In this paper, we propose a type of an enlarged Hilbert space, which enables us to construct a quantum simulator that simulates the original system set in such a way that a time-dependent weak (or modular) value in the original scheme is expressed as a one-way evolving expectation value in the enlarged scheme. This means that by causally running this simulator, we can simulate the time dependence of the weak value, which does not evolve causally but merely is a function of time t that will be known only after the postselection at the final time t_f.

The rest of this paper is organized as follows. In Sec. II, we introduce a mapping process of a given quantum state and an arbitrary state onto an enlarged state, and the dynamical evolution process of the enlarged system. Section III describes our main results. We apply the enlarged state of pre- and postselection states to the quantum weak and modular values and show that quantum weak and modular values can be expressed

*binho@qi.mp.es.oaska-u.ac.jp

as expectation values in the enlarged space. An example of a single spin under an external magnetic field is also given in this section. We also consider the case where the pre- and postselection states are mixed states. An experimental scheme for implementing the enlarged Hamiltonian is proposed in Sec. IV. We finally discuss and summarize our paper in Sec. V.

II. ENLARGED HILBERT SPACE METHOD

An *enlarged Hilbert space formalism* that can be implemented in a quantum simulator is a concept that has been proposed by Solano and his colleagues and has been extensively studied recently both theoretically and experimentally [27–36]. In this method, a given quantum state in a Hilbert space (usually named the *simulated space*) is embedded onto an enlarged state in an *enlarged Hilbert space*. Several manners of mapping have been suggested for different purposes. For example, a mapping that maps a pair of conjugate wave functions (ψ,ψ^*) onto an enlarged real wave function $\tilde{\psi}$ allows us to implement some unphysical operators, such as charge conjugation $\mathcal{C}$, parity inversion $\mathcal{P}$, and time reversal $\mathcal{T}$ [27–30]. It is also applicable to Majorana particles [27–29]. It is also successfully applied to measurements of the entanglement monotone [31–34]. Using another way of mapping, correlation functions in different reference frames, which are not directly measured, become observables that are directly measured [35]. A noncausal kinematic transformation and time or spatial parity transformations can also be discussed by an expectation value of the enlarged state [35,36].

In this section, we introduce a different way of mapping, where a given quantum state $\psi(t)$ is mapped together with an arbitrary state $\psi'(t)$, which we name as a *partner state*, onto an enlarged state $\Psi(t)$. We will choose, in the following section, the state that evolves from the initially prepared state as ψ and the state that backwardly evolves from the finally selected state as ψ'. For now, however, we stay in a general theory with arbitrary ψ and ψ'. Considering a given quantum state $|\psi(t)\rangle$ and its partner state $|\psi'(t)\rangle$ in an n-dimensional Hilbert space $\mathscr{H}_n$, these two states are mapped onto an enlarged state $|\Psi(t)\rangle$ in an enlarged Hilbert space $\mathbb{C}_2\otimes\mathscr{H}_n$. The mapping $\mathcal{M}:\mathscr{H}_n\to\mathbb{C}_2\otimes\mathscr{H}_n$, following [35], is

$$\psi(t)\xrightarrow{\mathcal{M}}\Psi(t)=\tfrac{1}{2}\{[\psi(t)+\psi'(t)],[\psi(t)-\psi'(t)]\}^{\boldsymbol{T}},\tag{2}$$

where $\boldsymbol{T}$ represents the transpose operation. Here we omit ket $|\,\rangle$ vectors for short. It is worthwhile to note that the mapping can be done by adding an extra qubit to the given system that contains the given state and its partner state. This mapping can always be implemented because any wave function can be expressed as

$$\psi(t)=\tfrac{1}{2}\{[\psi(t)+\psi'(t)]+[\psi(t)-\psi'(t)]\},\tag{3}$$

and therefore the quantum state can be decoded by the inverse $\psi(t)=\boldsymbol{M}\Psi(t)$, and the partner state is decoded by $\psi'(t)=\boldsymbol{M}(\boldsymbol{\sigma}_z\otimes\boldsymbol{I}_n)\Psi(t)$, where $\boldsymbol{M}\equiv(1,1)\otimes\boldsymbol{I}_n$, with $\boldsymbol{I}_n$ the n-dimensional identity matrix.

We now treat the dynamics of the Schrödinger equation in the enlarged Hilbert space. It should be noted that the quantum state satisfies the Schrödinger equation,

$$(i\partial_t-\boldsymbol{H})\psi(t)=0,\tag{4}$$

with the initial condition $\psi(t=0)$, and $\boldsymbol{H}$ is the system Hamiltonian in the original Hilbert space $\mathscr{H}_n$. We want to map this equation onto the one in the enlarged Hilbert space that satisfies

$$(i\partial_t-\tilde{\boldsymbol{H}})\Psi(t)=0,\tag{5}$$

as proposed in Ref. [31]. Here, $\tilde{\boldsymbol{H}}$ is the enlarged Hamiltonian in the enlarged Hilbert space $\mathbb{C}_2\otimes\mathscr{H}_n$. Following [31], if the state $\Psi(t)$ is the solution of Eq. (5) with the initial condition $\Psi(t=0)$, then the state $\boldsymbol{M}\Psi(t)$ is the solution of the Schrödinger equation (4) with the initial condition $\boldsymbol{M}\Psi(t=0)$. Here, in our mapping (2), they are both satisfied, i.e., $\psi(t=0)=\boldsymbol{M}\Psi(t=0)$ and $\psi(t)=\boldsymbol{M}\Psi(t)$. Therefore, if the condition $\boldsymbol{M}\tilde{\boldsymbol{H}}=\boldsymbol{H}\boldsymbol{M}$ is satisfied, Eq. (4) will be reproduced by operating $\boldsymbol{M}$ from the left of both sides of Eq. (5). With this condition, we obtain

$$\tilde{\boldsymbol{H}}=\begin{pmatrix}\boldsymbol{C}&\boldsymbol{B}\\ \boldsymbol{B}&\boldsymbol{C}\end{pmatrix}=\boldsymbol{I}_2\otimes\boldsymbol{C}+\boldsymbol{\sigma}_x\otimes\boldsymbol{B},\tag{6}$$

where $\boldsymbol{B}$ is an arbitrary $n\times n$ matrix and $\boldsymbol{C}\equiv\boldsymbol{H}-\boldsymbol{B}$, and $\boldsymbol{I}_2$ is the two-dimensional identity matrix.

Now, what will be the initial state of the enlarged expression? In fact, any $\Psi(0)$ that gives $\psi(0)=\boldsymbol{M}\Psi(0)$ is not enough. This is different from the case of [35] because here we can freely choose the partner state independent from the initial state of the system. Therefore, a proper choice would take into account the partner state at the initial time. The proper choice depends on each problem, and later we will show that we choose the initial partner state $\psi'(t=0)$ as the backwardly propagated state from the postselected state $\psi'(t_{\rm f})\equiv|\phi\rangle$.

III. QUANTUM WEAK AND MODULAR VALUES

Quantum weak value is a concept that was proposed by Aharonov *et al.* [4], where an expectation value of a given system observable is both depicted by the initial and final conditions. Most of the studies on weak values have focused on the interaction Hamiltonian between a quantum system and a measuring device for the case without the time evolution of the system. There were, however, a few studies on time-dependent weak values [37–40]. These studies, however, mainly focused on the time evolutions of the pre- and postselection states. There was a lack of discussion on how to measure (or obtain) time-dependent weak values (at least in principle). They instead mathematically consider the related effects caused by time-dependent weak values. Here, we also consider the evolution of the quantum system in describing the weak values and modular values. The main scope is to express them as expectation values evolving only by an enlarged initial condition in the enlarged system. Therefore, the enlarged weak values and modular values could be measured directly (measurements of expectation values) at the given time t.

A. Time-dependent weak values in a normal Hilbert space

We first consider a time-dependent weak value in a normal (i.e., not enlarged) Hilbert space. The process can be described as follows. A quantum system was prepared at time $t_{\rm i}$ in the identical quantum states $|\psi_{\rm i}(t_{\rm i})\rangle$, and a subensemble that is postselected in state $|\psi_{\rm f}(t_{\rm f})\rangle$ at time $t_{\rm f}$ with a given Hamiltonian

$\boldsymbol{H}$ takes place in the Hilbert space $\mathscr{H}_n$. In general, the postselected state does not need to be the freely evolved preselected state, i.e., $|\psi_{\rm f}(t_{\rm f})\rangle \neq |\psi_{\rm i}(t_{\rm f})\rangle$. The initial state propagates from time $t_{\rm i}$ by the unitary propagator $\boldsymbol{U}(t,t_{\rm i}) = \exp(-\frac{i}{\hbar}\int_{t_{\rm i}}^{t}\boldsymbol{H}d\tau)$ to time t ($> t_{\rm i}$) when the weak measurement is performed. Here, $\boldsymbol{H}$ is the free Hamiltonian of the system. The state just before the measurement is thus $\boldsymbol{U}(t,t_{\rm i})|\psi_{\rm i}(t_{\rm i})\rangle$. After weak interaction at time t, the system again evolves freely towards the final time $t_{\rm f}$ ($> t$) under the same propagator. The connection between the forward and backward evolutions is given by $\boldsymbol{U}(t_{\rm f},t) = \boldsymbol{U}^{-1}(t,t_{\rm f}) = \boldsymbol{U}^{\dagger}(t,t_{\rm f})$ [41]. Therefore, the final state of the system propagates toward the past with $\langle\psi_{\rm f}(t)| = \langle\psi_{\rm f}(t_{\rm f})|\boldsymbol{U}^{\dagger}(t,t_{\rm f})$. Then, the quantum weak value of a Hermitian operator $\boldsymbol{A}$ at time t ($t_{\rm i} < t < t_{\rm f}$), is expressed as

$$\langle\boldsymbol{A}(t)\rangle_{\rm w} = \frac{\langle\psi_{\rm f}(t_{\rm f})|\boldsymbol{U}^{\dagger}(t,t_{\rm f})|\boldsymbol{A}\boldsymbol{U}(t,t_{\rm i})|\psi_{\rm i}(t_{\rm i})\rangle}{\langle\psi_{\rm f}(t_{\rm f})|\boldsymbol{U}^{\dagger}(t,t_{\rm f})\boldsymbol{U}(t,t_{\rm i})|\psi_{\rm i}(t_{\rm i})\rangle}. \tag{7}$$

We next introduce "forward-evolving" and "backward-evolving" states at any time t, with $t_{\rm i} < t < t_{\rm f}$, that satisfy [23]

$$|\psi_{+}(t)\rangle = \boldsymbol{U}(t,t_{\rm i})|\psi_{\rm i}(t_{\rm i})\rangle, \tag{8a}$$

$$|\psi_{-}(t)\rangle = \boldsymbol{U}(t,t_{\rm f})|\psi_{\rm f}(t_{\rm f})\rangle, \tag{8b}$$

respectively. These expressions describe the forward evolution of the preselection state from $t_{\rm i}$ to t and the backward evolution of the postselection state from $t_{\rm f}$ to t, respectively. By using Eqs. (8), the weak value can be rewritten as follows:

$$\langle\boldsymbol{A}(t)\rangle_{\rm w} = \frac{\langle\psi_{-}(t)|\boldsymbol{A}|\psi_{+}(t)\rangle}{\langle\psi_{-}(t)|\psi_{+}(t)\rangle}. \tag{9}$$

It is notable that in the context of time-dependent weak values (and modular values), the choices of the pre- and postselected states are not relevant and even can be orthogonal, such as $\langle\psi_f(t_f)|\psi_i(t_i)\rangle = 0$. However, as can be seen from Eq. (9), the evolution states (the forward- and backward-evolving states) at any time t must be nonorthogonal. Also, for the enlarged state, it must be nonorthogonal to its "evolving state," i.e., $(\boldsymbol{\sigma}_z + i\boldsymbol{\sigma}_y)\otimes\boldsymbol{I}_n|\Psi(t)\rangle$ [see Eq. (12) below].

B. Time-dependent weak values in an enlarged Hilbert space: Expectation-value forms

Our primary purpose is to express weak values and modular values, which are defined with so-called two-state vector formalism, with single-state formalism such as expectation values. This can be done by embedding the forward-evolving and backward-evolving states onto an enlarged state by using our mapping method described in Sec. II. Indeed, the mapping (2) would give

$$\Psi(t) = \tfrac{1}{2}\{[\psi_{+}(t)+\psi_{-}(t)],[\psi_{+}(t)-\psi_{-}(t)]\}^{\boldsymbol{T}}, \tag{10}$$

where we have chosen $\psi(t) = \psi_{+}(t)$ and $\psi'(t) = \psi_{-}(t)$ in (2). Once again, we omit ket $|\ \rangle$ vectors for short. The forward-evolving and backward-evolving states, of course, can be decoded by

$$\psi_{+}(t) = \boldsymbol{M}\Psi(t) \text{ and } \psi_{-}(t) = \boldsymbol{M}(\boldsymbol{\sigma}_z\otimes\boldsymbol{I}_n)\Psi(t). \tag{11}$$

Then, the weak value in the enlarged Hilbert space is given, using Eqs. (9) and (11), as

$$\langle\boldsymbol{A}(t)\rangle_{\rm w} = \frac{\langle\Psi(t)|(\boldsymbol{\sigma}_z + i\boldsymbol{\sigma}_y)\otimes\boldsymbol{A}|\Psi(t)\rangle}{\langle\Psi(t)|(\boldsymbol{\sigma}_z + i\boldsymbol{\sigma}_y)\otimes\boldsymbol{I}_n|\Psi(t)\rangle}, \tag{12}$$

which completes the description of the weak value (of the system observable $\boldsymbol{A}$) by the time dependence of the enlarged state $|\Psi(t)\rangle$. Furthermore, the weak value now has the form of the *expectation value*, i.e., the ordinary single-state formalism for an enlarged system operator, $\boldsymbol{\sigma}_z\otimes\boldsymbol{A} + i\boldsymbol{\sigma}_y\otimes\boldsymbol{A}$. Note that although this operator is not a Hermitian operator, its expectation value is experimentally obtainable since it is a linear combination of two Hermitian operators. As a consequent, the time-dependent weak value can be dynamically obtained via the measurement of this expectation value.

This single-state formalism enables us to describe $\langle\boldsymbol{A}(t)\rangle_{\rm w}$, which originally requires the posterior condition $\psi_{\rm f}(t_{\rm f})$ to calculate, as a causal dynamics of the expectation value of the corresponding enlarged operator. The process is as follows. If an appropriate initial enlarged state is prepared at time $t_{\rm i}$ as $|\Psi(t_{\rm i})\rangle$, then it evolves to $|\Psi(t)\rangle$ under an appropriate enlarged evolution operator $\widetilde{\boldsymbol{U}}(t,t_{\rm i}) \equiv \exp(-\frac{i}{\hbar}\int_{t_{\rm i}}^{t}\widetilde{\boldsymbol{H}}d\tau)$. The weak value at time t then is given by the expectation value of the linear combination of Hermitian operators as above in Eq. (12). Of course, the enlarged evolution operator $\widetilde{\boldsymbol{U}}(t,t_{\rm i})$ should give the state evolution,

$$\Psi(\psi_{\rm i}(t_{\rm i}),\psi_{\rm f}(t_{\rm i}),t_{\rm i}) \xrightarrow{\widetilde{\boldsymbol{U}}(t,t_{\rm i})} \Psi(\psi_{\rm i}(t),\psi_{\rm f}(t),t). \tag{13}$$

For this $\psi_{\rm f}(t)$, the relation

$$|\psi_{\rm f}(t)\rangle = \boldsymbol{U}(t,t_{\rm f})|\psi_{\rm f}(t_{\rm f})\rangle \tag{14}$$

must also hold.

One possible way to satisfy both Eqs. (13) and (14) is to choose $\boldsymbol{B} = 0$ and $\boldsymbol{C} = \boldsymbol{H}$ in Eq. (6). Then the backward evolution $\boldsymbol{U}(t_{\rm i},t_{\rm f})|\psi_{\rm f}(t_{\rm f})\rangle$ satisfies the requirement and thus

$$|\psi_{\rm f}(t_{\rm i})\rangle = \boldsymbol{U}(t_{\rm i},t_{\rm f})|\psi_{\rm f}(t_{\rm f})\rangle. \tag{15}$$

Considering the case that we know both the system free evolution $\boldsymbol{U}(t_{\rm i},t_{\rm f})$ and the postselected state $|\psi_{\rm f}(t_{\rm f})\rangle$ beforehand, then $|\psi_{\rm f}(t_{\rm i})\rangle$ also becomes well defined at the initial time $t_{\rm i}$.

Note that other than $\boldsymbol{B} = 0$ and $\boldsymbol{C} = \boldsymbol{H}$, we can also freely choose $\boldsymbol{B}$ and $\boldsymbol{C}$ in Eq. (6). In this case, however, the backward evolution $\boldsymbol{U}(t_{\rm i},t_{\rm f})|\psi_{\rm f}(t_{\rm f})\rangle$ cannot satisfy the requirement, and we need more complicated calculations with the prior knowledge of postselected wave function at time t to determine the enlarged state $|\Psi(t_{\rm i})\rangle$.

C. Example

In this example, we illustrate a simple case where a spin operator of a spin-1/2 particle evolves under an external magnetic field applied along the z axis. The Hamiltonian and the evolution operator are given by

$$\boldsymbol{H} = \frac{\mu B}{2}\boldsymbol{\sigma}_z \quad\text{and}\quad \boldsymbol{U}(t) = e^{-\frac{i\omega t}{2}\boldsymbol{\sigma}_z}, \tag{16}$$

where μ and B are the amplitudes of the magnetic moment and the magnetic field, respectively, and $\omega = \frac{\mu B}{\hbar}$.

Suppose that we prepare an initial state, $|\uparrow_x\rangle$, which is a normalized eigenstate of Pauli matrix $\boldsymbol{\sigma}_x$,

$$|\psi_{\rm i}(t_{\rm i})\rangle = \frac{1}{\sqrt{2}}\begin{pmatrix}1\\1\end{pmatrix}, \tag{17}$$

with the bases $|\uparrow_z\rangle = \binom{1}{0}$ and $|\downarrow_z\rangle = \binom{0}{1}$. For the postselection at time $t_{\rm f}$, we consider three examples as the postselected states:

$$|\psi_{\rm f}(t_{\rm f})\rangle = \frac{1}{\sqrt{2}}\begin{pmatrix}1\\1\end{pmatrix}, \quad \frac{1}{\sqrt{2}}\begin{pmatrix}1\\-1\end{pmatrix}, \quad \text{and} \quad \frac{1}{\sqrt{2}}\begin{pmatrix}1\\i\end{pmatrix}, \tag{18}$$

which correspond to $|\uparrow_x\rangle$, $|\downarrow_x\rangle$, and $|\uparrow_y\rangle$, respectively. Let us choose $t_{\rm i} = 0$ and $t_{\rm f} = T$ for simplicity. Then the time-dependent weak values of $\boldsymbol{\sigma}_x$ calculated in the normal Hilbert space from Eq. (9) are

$${}_{\uparrow_x}\langle\boldsymbol{\sigma}_x\rangle^{\rm w}_{\uparrow_x} = \cos(\omega t) + \sin(\omega t)\tan\left(\frac{\omega T}{2}\right), \tag{19a}$$

$${}_{\downarrow_x}\langle\boldsymbol{\sigma}_x\rangle^{\rm w}_{\uparrow_x} = \cos(\omega t) - \sin(\omega t)\cot\left(\frac{\omega T}{2}\right), \tag{19b}$$

$${}_{\uparrow_y}\langle\boldsymbol{\sigma}_x\rangle^{\rm w}_{\uparrow_x} = \frac{\cos\left(\omega t - \frac{\omega T}{2} + \frac{\pi}{4}\right)}{\cos\left(\frac{\omega T}{2} - \frac{\pi}{4}\right)}. \tag{19c}$$

We next go through the same calculations in the enlarged Hilbert space. For simplicity, let us choose $\boldsymbol{B} = 0$ and $\boldsymbol{C} = \boldsymbol{H}$ in the decomposition $\boldsymbol{H} = \boldsymbol{B} + \boldsymbol{C}$. The corresponding Hamiltonian and the evolution operator in the enlarged space are

$$\tilde{\boldsymbol{H}} = \frac{\mu B}{2}\boldsymbol{I}^e \otimes \boldsymbol{\sigma}_z^s \quad \text{and} \quad \widetilde{\boldsymbol{U}}(t) = e^{-\frac{i\omega t}{2}\boldsymbol{I}^e\otimes\boldsymbol{\sigma}_z^s}, \tag{20}$$

where we have added superscripts e and s for the extra spin (ancilla qubit) and the system spin.

We also need to calculate the state $|\psi_{\rm f}(t_{\rm i})\rangle$ from the given $|\psi_{\rm f}(t_{\rm f})\rangle$, which can be done using Eq. (15) for each postselected state of Eq. (18). The initial enlarged state is then given as

$$|\Psi(t_{\rm i})\rangle = \frac{1}{2}\begin{pmatrix}|\psi_{\rm i}(t_{\rm i})\rangle + |\psi_{\rm f}(t_{\rm i})\rangle\\|\psi_{\rm i}(t_{\rm i})\rangle - |\psi_{\rm f}(t_{\rm i})\rangle\end{pmatrix}. \tag{21}$$

Under the enlarged evolution $\widetilde{\boldsymbol{U}}(t,t_{\rm i})$, this enlarged state evolves to $|\Psi(t)\rangle = \widetilde{\boldsymbol{U}}(t,t_{\rm i})|\Psi(t_{\rm i})\rangle$. Then the weak values obtained from Eq. (12) are the same as Eqs. (19). The detailed calculation is shown in Appendix A.

As an example case, when we choose $\omega T = \pi/2$, then the results of weak values are shown in Fig. 1. In general, the weak values depend on the measurement time. At $t = 0$, for all postselection cases, we get the results of weak values equal to 1, which means $\boldsymbol{\sigma}_x$ will be measured up regardless of postselection since the initial preparation state is $|\uparrow_x\rangle$, which is an eigenstate of $\boldsymbol{\sigma}_x$. As time t increases, the results will depend on both the pre- and postselection states at that time. For example, at $t = T/2$, the postselection onto $|\uparrow_x\rangle$ will give the maximum result of weak value (the red solid curve), which lies outside the range of $\boldsymbol{\sigma}_x$ eigenvalues $[-1, +1]$, while the postselected onto $|\downarrow_x\rangle$ will give the zero result (the green dashed curve), which means $\boldsymbol{\sigma}_x$ will be measured up or down with equal probability. Finally, for $t = T$, similar to the $t = 0$ case, the weak values depend on postselection states, for those

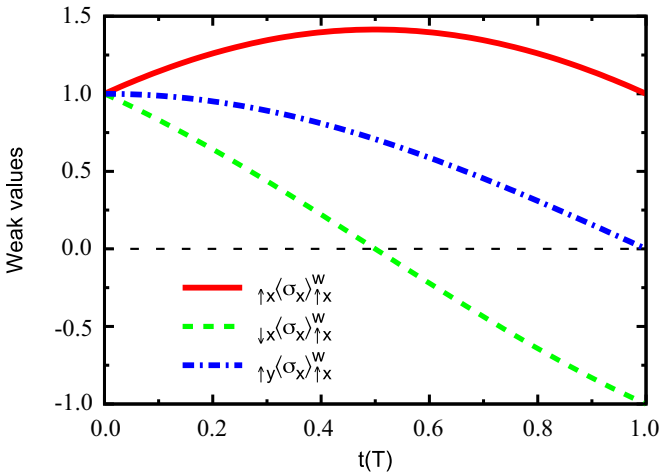

FIG. 1. Weak values of $\boldsymbol{\sigma}_x$ for the preselection state in (17) and various postselection states as in (18), which are the same in both cases of normal Hilbert space and enlarged Hilbert space.

are eigenstates of $\boldsymbol{\sigma}_x$ as we can see from the red and green curves for up and down orientations, respectively.

D. Time-dependent modular values in an enlarged Hilbert space

Another concept associated with the pre- and postselections is the modular value, which was first proposed by Kedem and Vaidman [5] and was recently studied by us [6,42,43]. For example, we have shown that by using the spectral decomposition, a modular value can be expressed regarding weak values [42] as

$$[\boldsymbol{A}(t)]_{\rm m} = \sum_i e^{-ig\lambda_i}\langle\boldsymbol{\Pi}_{a_i}(t)\rangle_{\rm w}, \tag{22}$$

where we have used $\boldsymbol{\Pi}_{a_i} = |a_i\rangle\langle a_i|$, and λ_i is one of the eigenvalues of the observable $\boldsymbol{A}$, i.e., $\boldsymbol{A} = \sum_i \lambda_i \boldsymbol{\Pi}_{a_i}$. This means that the modular value at time t is obtained by scanning and collecting all the weak values of the projection operators at this time. Fortunately, these weak values can be simultaneously measured at a given time by using such "scan-free method" that was introduced by Shi *et al.* [44]. As a result, time-dependent modular values in the enlarged Hilbert space can be determined via the time-dependent weak values.

E. Quantum weak and modular values with pre- and postselection density matrices

We consider that a "preselection" density matrix ρ propagates forward in time and a "postselection" density matrix E evolves backward in time. Let us assume that they are both represented by $n \times n$ complex density matrices. We introduce a mapping process from the original Hilbert space (n-dimensional) to an enlarged Hilbert space ($2n$-dimensional) that maps both ρ and E onto an enlarged density matrix. We define this enlarged density matrix at time t as follows:

$$\varrho_t = \frac{1}{2}\begin{pmatrix}\rho_t & 0_n\\0_n & E_t\end{pmatrix}, \tag{23}$$

where 0_n is the $n \times n$ zero matrix. The factor $1/2$ is used for normalization. Such a mapping can be implemented by adding

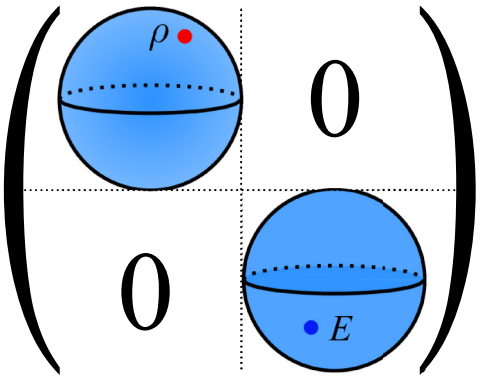

FIG. 2. A graphical illustration of the enlarged density matrix on the Bloch spheres. This representation is equivalent to the Majorana geometric representation in a sphere.

an ancillary qubit to the original system such that

$$\varrho_t = \tfrac{1}{2}[|0\rangle\langle 0| \otimes \rho_t + |1\rangle\langle 1| \otimes E_t], \tag{24}$$

where $|0\rangle \equiv \binom{1}{0}$ and $|1\rangle \equiv \binom{1}{0}$ are the chosen basis of the ancillary qubit. The original system density matrices can be decoded by the inversion,

$$\rho_t = 2\boldsymbol{M}\varrho_t\boldsymbol{N} \text{ and } E_t = 2\boldsymbol{M}\varrho_t(\boldsymbol{\sigma}_x \otimes \boldsymbol{I}_n)\boldsymbol{N}, \tag{25}$$

where again $\boldsymbol{M} = (1,1) \otimes \boldsymbol{I}_n$ while $\boldsymbol{N} = \binom{1}{0} \otimes \boldsymbol{I}_n$, and $\boldsymbol{I}_n$ is the $n \times n$ identity matrix. For illustration, we show a graphical matrix that contains the Bloch spheres that represent the pre- and postselection density matrices in Fig. 2.

Using this proposal, the weak value of a given observable $\boldsymbol{A}$ at any time t can be obtained from the enlarged density matrix ϱ_t as

$$\begin{aligned}\langle \boldsymbol{A}(t)\rangle_{\rm w} &\equiv \frac{{\rm Tr}[E_t \boldsymbol{A}\rho_t]}{{\rm Tr}[E_t\rho_t]} \\ &= \frac{{\rm Tr}[\boldsymbol{M}\varrho_t(\boldsymbol{\sigma}_x \otimes \boldsymbol{I}_n)\boldsymbol{N}\ \boldsymbol{A}\ \boldsymbol{M}\varrho_t\boldsymbol{N}]}{{\rm Tr}[\boldsymbol{M}\varrho_t(\boldsymbol{\sigma}_x \otimes \boldsymbol{I}_n)\boldsymbol{N}\ \boldsymbol{M}\varrho_t\boldsymbol{M}]},\end{aligned} \tag{26}$$

where we have submitted ρ_t and E_t from Eq. (25). A similar result can be drawn for the case of modular values.

IV. IMPLEMENTATION OF ENLARGED HILBERT SPACES

In this section, we discuss how to implement the evolution associated with the enlarged Hamiltonian by a real quantum simulator. In many cases, a Hamiltonian to be simulated is expressed by a many-body-system Hamiltonian, which is the summation of the subsystems Hamiltonians. So, we assume that the enlarged Hamiltonian is expressed as $\tilde{\boldsymbol{H}} = \sum_j \tilde{\boldsymbol{H}}_j$, where $\tilde{\boldsymbol{H}}_j$ are in general nonlocal and noncommuting operators. Using the Trotter technique [45,46], the evolution operator is expressed as

$$\widetilde{\boldsymbol{U}} = e^{-\frac{i}{\hbar}\sum_j \tilde{\boldsymbol{H}}_j t} \simeq \left(\prod_j e^{-\frac{i}{\hbar}\tilde{\boldsymbol{H}}_j t/k}\right)^k, \tag{27}$$

where k is the number of Trotter steps. If $\tilde{\boldsymbol{H}}_j$ are local Hamiltonians, the evolution process can be implemented

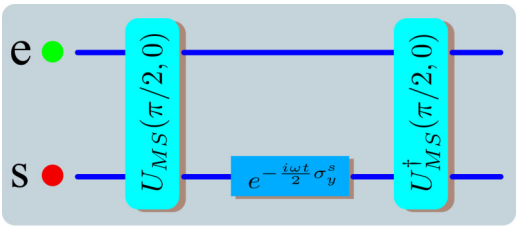

FIG. 3. A scheme of gates on both the extra spin (e) and the system single-particle spin (s).

by using a "genetic algorithm" for digital quantum simulations [47]. Here, however, we assume that $\tilde{\boldsymbol{H}}_j$ are nonlocal, so the genetic algorithm is not applicable. Fortunately, however, each $\tilde{\boldsymbol{H}}_j$ is decomposed into tensor products of Pauli matrices [32,48]. In this case, $e^{-\frac{i}{\hbar}\tilde{\boldsymbol{H}}_j t/k}$ can be implemented by using nonlocal entangling Mølmer-Sørensen gates $\boldsymbol{U}_{\rm MS}(\theta,\phi) = \exp[-i\frac{\theta}{4}(\cos\phi\boldsymbol{S}_x + \sin\phi\boldsymbol{S}_y)^2]$, and local single-qubit rotations (see Refs. [32,48]), where the operators $\boldsymbol{S}_{x,y} = \sum_{i=1}^N \boldsymbol{\sigma}_{x,y}^i$, θ and ϕ are two angle parameters, and N is the number of local qubits [49,50].

We now apply the above method to our enlarged Hamiltonian (6). Here we adopt a situation that an n-dimensional Hamiltonian $\boldsymbol{H}$ is realized by a (nonlocal) N-qubit system, where $n = 2^N$. In most cases, as was discussed in Sec. II and will be discussed in this section, an N-body system in the original Hilbert space can be expressed by an $(N+1)$-body interaction in the enlarged Hilbert space. This means that the quantum simulation in the enlarged space is realized by adding one extra qubit to the original system [31,35]. Then we have

$$\tilde{\boldsymbol{H}} = \boldsymbol{I}_2^e \otimes \boldsymbol{C}^s + \boldsymbol{\sigma}_x^e \otimes \boldsymbol{B}^s = \sum_{j=1}^2 \tilde{\boldsymbol{H}}_j, \tag{28}$$

where $\tilde{\boldsymbol{H}}_1 \equiv \boldsymbol{I}_2^e \otimes \boldsymbol{C}^s$ and $\tilde{\boldsymbol{H}}_2 \equiv \boldsymbol{\sigma}_x^e \otimes \boldsymbol{B}^s$. We assume that both $\boldsymbol{B}^s$ and $\boldsymbol{C}^s$ can be decomposed into tensor products of N Pauli matrices. We then use the Trotter technique to decompose the total evolution operator as

$$\widetilde{\boldsymbol{U}} = e^{-igt\sum_j \tilde{\boldsymbol{H}}_j} = \left(\prod_{j=1}^2 e^{-igt\tilde{\boldsymbol{H}}_j/k}\right)^k, \tag{29}$$

where g is the coupling constant of the simulated system. The evolution corresponding to $j = 1$ can be implemented easily by using single-qubit rotations. For $j = 2$, the evolution can be implemented (see Fig. 3) as follows:

(i) Operate a Mølmer-Sørensen entangling gate, $\boldsymbol{U}_{\rm MS}(\theta,\phi)$, to all $(N+1)$ qubits.

(ii) Apply a local single-qubit gate, $\exp(-i\frac{\varphi}{2}\boldsymbol{\sigma}_\gamma^e \otimes \boldsymbol{I}_{2^N}^s)$, to the extra qubit. Here, the phase φ is designed by controlling $2gt$ and γ is chosen from x, y, or z, depending on the parity (odd or even) of N [48].

(iii) The total system is reversed by the inverse entangling gate $\boldsymbol{U}_{\rm MS}^\dagger$.

This sequence (i)–(iii) can be summarized as

$$\boldsymbol{U}_{\rm MS} e^{-igt\boldsymbol{\sigma}_\gamma^e \otimes \boldsymbol{I}_{2^N}^s} \boldsymbol{U}_{\rm MS}^\dagger, \tag{30}$$

and can implement the desired enlarged evolution $\widetilde{\boldsymbol{U}}$ in Eq. (29).

As an example, let us apply this method to the case of the example in Sec. III C, where we consider the case $\tilde{\boldsymbol{H}} = \frac{\mu B}{2}\boldsymbol{\sigma}_x^e \otimes \boldsymbol{\sigma}_z$ [i.e., $j = 2$ in Eq. (28)]. The evolution $\widetilde{\boldsymbol{U}} = \exp(-\frac{i\omega t}{2}\boldsymbol{\sigma}_x^e \otimes \boldsymbol{\sigma}_z^s)$ can be calculated (see Appendix B) as

$$\widetilde{\boldsymbol{U}} = \boldsymbol{U}_{\rm MS}\left(\frac{\pi}{2},0\right)e^{-\frac{i\omega t}{2}\boldsymbol{I}_2^e\otimes\sigma_y^s}\boldsymbol{U}_{\rm MS}\left(-\frac{\pi}{2},0\right), \tag{31}$$

where the Mølmer-Sørensen gates $\boldsymbol{U}_{\rm MS}(\pi/2,0)$ and $\boldsymbol{U}_{\rm MS}^{\dagger}(\pi/2,0)$ act on both the extra spin and the system single-particle spin. Here, there is a slight difference from Eq. (30): we apply the single-spin rotation onto the system spin, where it is simpler for this particular example. The process can be seen from Fig. 3. We also emphasize that such gates can be simulated by a physical system, such as ion traps [27,51–53], quantum photonics, superconducting circuits, and others (see [54]).

V. DISCUSSION AND CONCLUSION

It is also worthwhile to note that recently, Vaidman *et al.* have claimed that weak values are eigenvalues, rather than expectation values [55]. In their work, the authors mainly consider the Bures angle of the two measuring-device states as the distance between them [55],

$$D_A(\Phi_e,\Phi_w) \equiv \arccos|\langle\Phi_e|\Phi_w\rangle|, \tag{32}$$

where Φ_e is the final measuring-device state corresponding to the "eigenvalues" case, and the final measuring-device state Φ_w corresponds to the "weak values" case. The authors show that $D_A(\Phi_e,\Phi_w)$ can be neglected, which typically means weak values are very close to eigenvalues, rather than expectation values. Their conclusion seems to conflict with our results here. However, if we note that their work was done in the same Hilbert space, then we can claim that there is no conflict at all because, in our work, we show that weak values in the normal Hilbert space become expectation values in the enlarged Hilbert space. Moreover, of course, if we reduce from the enlarged Hilbert space to normal Hilbert space, then the expectation values will come back to the standard weak values, which are described by both pre- and postselection states.

In conclusion, we showed that the time dependence of a quantum weak value and that of a modular value, which are expressed by the two-state vector formalism, can be interpreted as the expectation values of a linear combination of operators in the enlarged Hilbert space. Therefore, if such enlarged Hilbert space is realized by a new experimental setup, the weak and modular values in the original problem are obtained merely by direct measurements of the (enlarged) observables and calculating its expectation value. This formalism enables us to trace the causal evolution of the enlarged observable instead of considering the weak or modular values by the original initial-final-state problem. Some examples are also given in this paper.

ACKNOWLEDGMENTS

This work was supported by CREST, JST Grant No. JPMJCR1671 and JSPS Grant-in-Aid for Scientific Research(A) No. JP16H02214.

APPENDIX A: WEAK VALUES IN THE ENLARGED HILBERT SPACE

In this Appendix, we will show how to calculate the weak value of $\boldsymbol{\sigma}_x$ in the enlarged Hilbert space. For example, we assume that the pre- and postselection states are both $|\uparrow_x\rangle$, but other cases can be treated similarly. We first calculate the postselection state at time $t_{\rm i} = 0$ (we also choose $t_{\rm f} = T$),

$$\begin{aligned}|\psi_{\rm f}(0)\rangle &= \boldsymbol{U}(0,T)|\psi_{\rm f}(T)\rangle\\ &= e^{\frac{i\omega T}{2}\boldsymbol{\sigma}_z}\frac{1}{\sqrt{2}}\begin{pmatrix}1\\1\end{pmatrix}\\ &= \frac{1}{\sqrt{2}}\begin{pmatrix}e^{\frac{i\omega T}{2}}\\e^{-\frac{i\omega T}{2}}\end{pmatrix}.\end{aligned} \tag{A1}$$

The enlarged state at time $t_{\rm i} = 0$ is given by

$$|\Psi(0)\rangle = \frac{1}{2\sqrt{2}}\begin{pmatrix}1+e^{\frac{i\omega T}{2}}\\1+e^{-\frac{i\omega T}{2}}\\1-e^{\frac{i\omega T}{2}}\\1-e^{-\frac{i\omega T}{2}}\end{pmatrix}. \tag{A2}$$

Under the evolution given by Eq. (20), the enlarged state evolves according to

$$\begin{aligned}|\Psi(t)\rangle &= \widetilde{\boldsymbol{U}}(t,0)|\Psi(0)\rangle\\ &= \frac{1}{2\sqrt{2}}\begin{pmatrix}e^{-\frac{i\omega t}{2}}\left(1+e^{\frac{i\omega T}{2}}\right)\\e^{\frac{i\omega t}{2}}\left(1+e^{-\frac{i\omega T}{2}}\right)\\e^{-\frac{i\omega t}{2}}\left(1-e^{\frac{i\omega T}{2}}\right)\\e^{\frac{i\omega t}{2}}\left(1-e^{-\frac{i\omega T}{2}}\right)\end{pmatrix}.\end{aligned} \tag{A3}$$

Then the weak value of $\boldsymbol{\sigma}_x$, which is given by Eq. (12), yields

$$\begin{aligned}{}_{\uparrow_x}\langle\boldsymbol{\sigma}_x\rangle_{\uparrow_x}^{\rm w} &= \frac{\langle\Psi(t)|(\boldsymbol{\sigma}_z+i\boldsymbol{\sigma}_y)\otimes\boldsymbol{\sigma}_x|\Psi(t)\rangle}{\langle\Psi(t)|(\boldsymbol{\sigma}_z+i\boldsymbol{\sigma}_y)\otimes\boldsymbol{I}_2|\Psi(t)\rangle}\\ &= \cos(\omega t)+\sin(\omega t)\tan\left(\frac{\omega T}{2}\right),\end{aligned} \tag{A4}$$

which is the same result as Eq. (19a) in the main text.

APPENDIX B: AN IMPLEMENTATION OF THE EXAMPLE OF SINGLE SPIN

In this part, we will show how to implement the evolution

$$\widetilde{\boldsymbol{U}}(t) = e^{-\frac{i\omega t}{2}\boldsymbol{\sigma}_x^e\otimes\boldsymbol{\sigma}_z^s}, \tag{B1}$$

by using two Mølmer-Sørensen gates and a local rotation gate. We start from two Mølmer-Sørensen gates applied onto both the extra spin and the system spin and one local rotation gate

applied on the system spin only (see Fig. 3),

$$\boldsymbol{U}_{\rm MS}(\theta,\phi)e^{-\frac{i\omega t}{2}\boldsymbol{\sigma}_y^s}\boldsymbol{U}_{\rm MS}^\dagger(\theta,\phi)=e^{-\frac{i\omega t}{2}\boldsymbol{U}_{\rm MS}(\theta,\phi)\boldsymbol{\sigma}_y^s\boldsymbol{U}_{\rm MS}^\dagger(\theta,\phi)}. \quad \text{(B2)}$$

Here, we have used the useful formula $\boldsymbol{U}e^{\boldsymbol{H}}\boldsymbol{U}^\dagger=e^{\boldsymbol{U}\boldsymbol{H}\boldsymbol{U}^\dagger}$ [56], $\boldsymbol{U}_{\rm MS}(\theta,\phi)=e^{-\frac{i\theta}{4}(\cos\phi\boldsymbol{S}_x+\sin\phi\boldsymbol{S}_y)^2}$, $\boldsymbol{S}_{x,y}=\sum_{k=1}^K\boldsymbol{\sigma}_{x,y}^k$, and K is the number of qubits that the Mølmer-Sørensen gate is acting on. In our case, $K=2$ and $\phi=0$, which lead to

$$\boldsymbol{U}_{\rm MS}(\theta,0)=e^{-\frac{i\theta}{4}(\boldsymbol{\sigma}_x^e+\boldsymbol{\sigma}_z^s)^2}. \quad \text{(B3)}$$

Then the term $\boldsymbol{U}_{\rm MS}(\theta,\phi)\boldsymbol{\sigma}_y^s\boldsymbol{U}_{\rm SM}^\dagger(\theta,\phi)$ in Eq. (B2) is calculated to be

$$\begin{aligned}\boldsymbol{U}_{\rm MS}(\theta,\phi)\boldsymbol{\sigma}_y^s\boldsymbol{U}_{\rm MS}^\dagger(\theta,\phi)&=e^{-\frac{i\theta}{4}(\boldsymbol{\sigma}_x^e+\boldsymbol{\sigma}_z^s)^2}\boldsymbol{\sigma}_y^s e^{\frac{i\theta}{4}(\boldsymbol{\sigma}_x^e+\boldsymbol{\sigma}_z^s)^2}\\&=\cos\theta\boldsymbol{\sigma}_y^s+\sin\theta\boldsymbol{\sigma}_x^e\boldsymbol{\sigma}_z^s, \quad \text{(B4)}\end{aligned}$$

where we have used the Baker-Campbell-Hausdorff relation $e^{\boldsymbol{A}}\boldsymbol{B}e^{-\boldsymbol{A}}=\boldsymbol{B}+[\boldsymbol{A},\boldsymbol{B}]+\frac{1}{2!}[\boldsymbol{A},[\boldsymbol{A},\boldsymbol{B}]]+\cdots$. Then with the choice of $\theta=\pi/2$, Eq. (B2) reduces to Eq. (B1), which is the result in Eq. (31).

[1] Y. Aharonov and L. Vaidman, J. Phys. A **24**, 2315 (1991).
[2] *Potentiality, Entanglement and Passion-at-a-Distance*, Quantum Mechanical Studies for A. M. Shimony, edited by R. S. Cohen, M. Horne, and J. J. Stachel (Kluwer Academic, The Netherlands, 1997).
[3] *Time in Quantum Mechanics*, 2nd ed., edited by J. G. Muga, R. S. Mayato, and I. Egusquiza (Springer, New York, 2007).
[4] Y. Aharonov, D. Z. Albert, and L. Vaidman, Phys. Rev. Lett. **60**, 1351 (1988).
[5] Y. Kedem and L. Vaidman, Phys. Rev. Lett. **105**, 230401 (2010).
[6] L. B. Ho and N. Imoto, Phys. Lett. A **380**, 2129 (2016).
[7] Y. Aharonov and D. Rohrlich, *Quantum Paradoxes: Quantum Theory for the Perplexed* (Weinheim: Wiley-VCH, New York, 2005), Chap. 17.
[8] Y. Aharonov, S. Nussinov, S. Popescu, and L. Vaidman, Phys. Rev. A **87**, 014105 (2013).
[9] L. Hardy, Phys. Rew. Lett. **68**, 2981 (1992).
[10] Y. Aharonov, A. Botero, S. Popescu, B. Rezink, and J. Tollaksen, Phys. Lett. A **301**, 130 (2002).
[11] J. S. Lundeen and A. M. Steinberg, Phys. Rev. Lett. **102**, 020404 (2009).
[12] K. Yokota, T. Yamamoto, M. Koashi, and N. Imoto, New J. Phys. **11**, 033011 (2009).
[13] Y. Aharonov, S. Popescu, D. Rohrlich, and P. Skrzypczky, New J. Phys. **15**, 113015 (2013).
[14] T. Denkmayr, H. Geppert, S. Sponar, H. Lemmel, A. Matzkin, J. Tollaksen, and Y. Hasegawa, Nat. Commun. **5**, 4492 (2014).
[15] H. F. Hofmann, Phys. Rev. A **89**, 042115 (2014).
[16] S. Pang, J. Dressel, and T. A. Brun, Phys. Rev. Lett. **113**, 030401 (2014).
[17] L. Zhang, A. Datta, and I. A. Walmsley, Phys. Rev. Lett. **114**, 210801 (2015).
[18] S. Huang and G. S. Agarwal, New J. Phys. **17**, 093032 (2015).
[19] A. Nishizawa, Phys. Rev. A **92**, 032123 (2015).
[20] Y. Susa and S. Tanaka, Phys. Rev. A **92**, 012112 (2015).
[21] I. M. Duck, P. M. Stevenson, and E. C. G. Sudarshan, Phys. Rev. D **40**, 2112 (1989).
[22] J. Dressel, M. Malik, F. M. Miatto, A. N. Jordan, and R. W. Boyd, Rev. Mode. Phys. **86**, 307 (2014).
[23] B. Reznik and Y. Aharonov, Phys. Rev. A **52**, 2538 (1995).
[24] Y. Shikano and A. Hosoya, J. Phys. A **43**, 025304 (2010).
[25] R. Silva, Y. Guryanova, A. J. Short, P. Skrzypczyk, N. Brunner, and S. Popescu, New J. Phys. **19**, 103022 (2017).
[26] O. Oreshkov and C. Giarmatzi, New J. Phys. **18**, 093020 (2016).
[27] J. Casanova, C. Sabin, J. Leon, I. L. Egusquiza, R. Gerritsma, C. F. Roos, J. J. Garcia-Ripoll, and E. Solano, Phys. Rev. X **1**, 021018 (2011).
[28] C. Noh, B. M. Rodriguez-Lara, and D. G. Angelakis, Phys. Rev. A **87**, 040102(R) (2013).
[29] B. M. Rodriguez-Lara and H. M. Moya-Cessa, Phys. Rev. A **89**, 015803 (2014).
[30] X. Zhang, Y. Shen, J. Zhang, J. Casanova, L. Lamata, E. Solano, M.-H. Yung, J.-N. Zhang, and K. Kim, Nat. Commun. **6**, 7917 (2015).
[31] R. DiCandia, B. Mejia, H. Castillo, J. S. Pedernales, J. Casanova, and E. Solano, Phys. Rev. Lett. **111**, 240502 (2013).
[32] J. S. Pedernales, R. DiCandia, P. Schindler, T. Monz, M. Hennrich, J. Casanova, and E. Solano, Phys. Rev. A **90**, 012327 (2014).
[33] J. C. Loredo, M. P. Almeida, R. Di Candia, J. S. Pedernales, J. Casanova, E. Solano, and A. G. White, Phys. Rev. Lett. **116**, 070503 (2016).
[34] M. C. Chen, D. Wu, Z. E. Su, X. D. Cai, X. L. Wang, T. Yang, L. Li, N. L. Liu, C. Y. Lu, and J. W. Pan, Phys. Rev. Lett. **116**, 070502 (2016).
[35] U. Alvarez-Rodriguez, J. Casanova, L. Lamata, and E. Solano, Phys. Rev. Lett. **111**, 090503 (2013).
[36] X. H. Cheng, U. Alvarez-Rodriguez, L. Lamata, X. Chen, and E. Solano, Phys. Rev. A **92**, 022344 (2015).
[37] A. D. Parks, J. Phys. A **41**, 335305 (2008).
[38] P. C. W. Davies, Phys. Rev. A **79**, 032103 (2009).
[39] M. Ban, J. Mod. Phys. **4**, 1 (2013).
[40] Y. Aharonov, E. Cohen, A. Landau, and A. C. Elitzur, Sci. Rep. **7**, 531 (2017).
[41] Y. Aharonov, E. Cohen, and A. C. Elitzur, Ann. Phys. **355**, 258 (2015).
[42] L. B. Ho and N. Imoto, arXiv:1602.01594v2.
[43] L. B. Ho and N. Imoto, Phys. Rew. A **95**, 032135 (2017).
[44] Z. Shi, M. Mirhosseine, J. Margiewicz, M. Malik, F. Rivera, Z. Zhu, and W. Boyd, Optica **2**, 388 (2015).
[45] H. F. Trotter, Proc. Am. Math. Soc. **10**, 545 (1959).
[46] S. Lloyd, Science **273**, 1073 (1996).
[47] U. LasHeras, U. Alvarez-Rodriguez, E. Solano, and M. Sanz, Phys. Rev. Lett. **116**, 230504 (2016).
[48] J. Casanova, A. Mezzacapo, L. Lamata, and E. Solano, Phys. Rev. Lett. **108**, 190502 (2012).
[49] K. Mølmer and A. Sørensen, Phys. Rev. Lett. **82**, 1835 (1999).

[50] M. Müller, K. Hammerer, Y. L. Zhou, C. F. Roos, and P. Zoller, New J. Phys. **13**, 085007 (2011).
[51] D. Leibfried, R. Blatt, C. Monroe, and D. Wineland, Rev. Mod. Phys. **75**, 281 (2003).
[52] R. Batt and C. F. Roos, Nat. Phys. **8**, 277 (2012).
[53] L. Lamata, A. Mezzacapo, J. Casanova, and E. Solano, EPJ Quantum Technol. **1**, 9 (2014).
[54] I. M. Georgescu, S. Ashhab, and F. Nori, Rev. Mod. Phys. **86**, 153 (2014).
[55] L. Vaidman, A. Ben-Israel, J. Dziewior, L. Knips, M. Weissl, J. Meinecke, C. Schwemmer, R. Ber, and H. Weinfurter, Phys. Rev. A **96**, 032114 (2017).
[56] W. Dür, M. J. Bremner, and H. J. Briegel, Phys. Rev. A **78**, 052325 (2008).